

# Site preference of Fe atoms in olivine, $(\text{Fe}_x\text{Mg}_{2-x})\text{SiO}_4$ , and on its surface

Ming Geng\*

*Science Institute, University of Iceland, VR-III, Reykjavík 107, Iceland and  
Center for Earth Evolution and Dynamics (CEED), University of Oslo, Norway*

Hannes Jónsson†

*Science Institute, University of Iceland, VR-III, Reykjavík 107, Iceland*

(Dated: July 11, 2023)

Olivine is involved in many natural reactions and industrial reactions as a catalyst. The catalytic ability is highly possible rely on the  $\text{Fe}^{2+}$  in olivine. We use density functional theory calculation and thermodynamics to investigate the site preference of the Fe atom in olivine which composition from iron-rich to iron-poor and its surfaces. The  $\text{Fe}^{2+}$  always shows its high spin (quintet) state which has a larger ion radius than  $\text{Mg}^{2+}$  in olivine crystals and surfaces. The  $\text{Fe}^{2+}$  inside the surface slab prefers the smaller M1 site than M2 site by enlarging the metal-oxygen octahedra when occupied the metal site as in the bulk system. Energy contribution of entropy accumulation caused temperature raise stops this preference at the temperature where a cation order-disorder distribution energy crossover happens in olivine. Surface exposed sites provide  $\text{Fe}^{2+}$  large space due to its unsaturated nature. This leads to a higher level of preference of  $\text{Fe}^{2+}$  to the surface site than any metal site inside the crystal no matter M1 or M2 site is exposed. This indicates the  $\text{Fe}^{2+}$  in the bulk system can diffuse to a metal site exposed on the surface driven by the energy difference. Many reactions can use the on-surface  $\text{Fe}^{2+}$  as a catalyst because of the active chemical behaviour of Fe. Meanwhile, this energetic preference should be considered in the future model to explain the naturally observed zoning olivine have a high Fe edge and low Fe center. These microscopic understanding can be essential to many olivine related geochemical and astrochemical reactions.

## I. INTRODUCTION

Olivine, a magnesium-iron silicate mineral  $(\text{Mg}_x\text{Fe}_{2-x})\text{SiO}_4$  ( $x = 0 - 2$ ), is the predominant mineral in both the Earth's upper mantle and interstellar media in space. Consequently, knowledge of the physical and chemical properties of olivine is of great geophysical and astrochemical interest because of its role in many important processes [1–5]. Olivine forms a solid solution series between the fayalite, iron end member ( $\text{Fe}_2\text{SiO}_4$ ), and forsterite, the magnesium end member ( $\text{Mg}_2\text{SiO}_4$ ). Fo value (forsterite percentage) usually used for describing the composition of the mineral in the solution, such as Fo50 means the olivine with 50% of forsterite and 50% fayalite. Olivine crystals have an orthorhombic structure with the space group  $Pbmn$  each Si atom in olivine coordinates with four O atoms to form a  $[\text{SiO}_4]$  tetrahedron, while each (Mg, Fe) atom are surrounded by 6 O atoms in two types of inequivalent metal site, one on the plane of mirror symmetry (M2 site) and the other on the inversion center (M1 site) as shown in Figure.1. Forsterite transforms to spinel structure minerals, wadsleyite ( $Imma$ ) and ringwoodite ( $Fd3m$ ), in mantle transition zone with pressure upon to  $\sim 13.5\text{GPa}$  and  $\sim 18\text{GPa}$  [6], respectively. Fayalite directly transforms to spinel structure at  $8\text{GPa}$ [7]. The natural olivine lays on a mixer of the Fe-Mg solid solution would expect to transform to spinel structure

between  $13.5\text{GPa}$  and  $8\text{GPa}$  corresponding to the iron concentration based on thermodynamics mixing laws. Even with the same iron concentration, the distribution of Fe and Mg atoms also affects the physical and chemical properties of the mineral[8]. Since  $\text{Fe}^{2+}$  has a more complex electronic configuration than  $\text{Mg}^{2+}$ , thus olivine with iron may lead more interesting chemistry than pure magnesium forsterite towards the reactivity of the fluid molecules in touch with a surface of the olivine if the  $\text{Fe}^{2+}$  happen to expose on the surface which many catalysis studies have proved[4, 9]. On the other hand, the  $3d^6$  in  $\text{Fe}^{2+}$  also poses challenges due to the interplay of charge and spin at the Fe site. The first thing that needs to know is the  $\text{Fe}^{2+}$  distribution in the surface slab which is very difficult to investigate in experiments. Therefore combining the surface structure and  $\text{Fe}^{2+}$  distribution in bulk is needed in further understanding these catalytic processes.

In some geophysical theoretic models, the  $\text{Fe}^{2+}$  distribution over M1 and M2 sites were described using the value of a distribution coefficient( $k_D$ )

$$k_D = \frac{Fe^{M1} \cdot Mg^{M2}}{Fe^{M2} \cdot Mg^{M1}} \quad (1)$$

which  $Fe^{M1}$  and  $Mg^{M1}$  are atomic fractions of  $\text{Fe}^{2+}$  and  $\text{Mg}^{2+}$  in M1 site, similar for M2 site. The  $k_D$  larger than 1 is considered the Fe atom prefers more to the M1 site. Some mantle seismic discontinuities are considered to be related to the  $k_D$  of olivine[10]. Observation found that olivines form the plutonic and metamorphic rocks have a roughly equal  $\text{Fe}^{2+}$  and  $\text{Mg}^{2+}$  in both M1 and M2 sites[11]. Meanwhile, Moon's olivines and those

\* gengm@hi.is

† hj@hi.is

from volcanic terrestrial rock seems to be a weak preference of  $Fe^{2+}$  for M1 site. These observations indicate the different evolution processes can lead different cation distributions when natural olivine crystallization. Studies in Li-ion batteries trying to utilise the multivalent ion rather than monovalent to improve the energy density of the battery. Since  $(Mg,Fe)_2SiO_4$  has the same structure as the  $LiFePO_4$ , the  $(Mg,Fe)_2SiO_4$  also become a strong candidate of new battery cathode material. The orderer phase of  $MgFeSiO_4$  structure have been synthesised through high temperature methods. However, the ordering distribution of Mg and Fe in the olivine which is the fundamental part to consider the possible ion diffusion mechanism is not clear yet.

In experimental studies, various results were conducted from different methods on the distribution of  $Fe^{2+}$ . It was found by many studies olivines shows a weak ordering distribution of  $Mg^{2+}$ ,  $Fe^{2+}$  at high temperature and numerous quenching experiments.[12–15] Most experimental results were obtained by X-ray diffraction or Mössbauer spectroscopy and these methods are poorly applicable to vast majority of natural olivines due to nearly all mantle olivines fall in Fo89 to Fo94[16] which have a relatively low iron content. Two Mössbauer doublets caused by  $Fe^{2+}$  in M1 and M2 sites are very close to each other by both isometric shift and quadrupole splitting thus strongly overlapping in the spectra. New methods such as polarized near-infrared optical absorption spectroscopy [17] and paramagnetically shifted NMR [18] were tested to determine the site preference of the transition metal especially  $Fe^{2+}$  in the olivine. Unfortunately, experimental results failed to reach a common conclusion. Atomic simulation of mineral crystals and surfaces become a useful method to investigate the mineral in extreme pressure temperature conditions as in the Earth's interior, surface structure and electron properties due to the difficulties in experimental research. Most theoretical studies are focused on the end members, some particular properties are investigated on certain iron concentrations. Chartterjee et al.[19] compared  $Fe^{2+}$  M1 and M2 in Fo50, whereas the natural olivines have a much higher Fo which means less iron content. A slight preference for M1 site of  $Fe^{2+}$  was found in their calculation result. Das et al.[8] compared two types of cation ordering Fo50 olivine elastic properties. Javier et al.[20] is the only study that compared pure magnesium forsterite and one iron containing olivine(Fo75) surface with B3LYP functional, but the cation site difference is not discussed in the study. A systematic analysis of the distribution of cations in olivine and its surface is needed to establish an ion diffusion mechanism and surface reactivity. A surface slab can be approximated as two exposed surfaces layer and a block of bulk system. In our work, we investigated the  $Fe^{2+}$  distribution both in bulk and surface system in the same schema and combine them together, so we can get the  $Fe^{2+}$  preference in a slab.

In this article, we present simulations of  $(Mg_xFe_{2-x})SiO_4$  with several Fe concentrations in

bulk and its surface to analyze the energy preference of the Fe atoms distribution in the material using Density functional theory (DFT) calculations. Section II will describe the crystal and surface structure and computation detail. In section III, the results obtained are presented with some discussion. The conclusion is summarized in section IV.

## II. METHODS

### A. Crystal and Surface structures

Like many silicate minerals, olivine is essentially built out of  $SiO_4$  tetrahedra blocks. The tetrahedra units are isolated from each other and this type of mineral is called nesosilicates. The unit cell contains 4 formula units, 4 Si, 16 O atoms and 8 metal atoms. With the oxygen atoms on the tetrahedra corners, two types of octahedra also formed of which metal cations sites  $M1$  and  $M2$  are located in the center as shown in Figure.1. The  $M1O_6$  octahedra units are connected to each other like a chain by sharing a  $O - O$  edge formed by two oxygen different oxygen atoms.  $M2O_6$  octahedra units are connected by sharing two equivalence oxygen atoms to form a plane parallel to ac face of the unit cell. At room temperature, the  $M1$  site is slightly more distorted than  $M2$  [21]. So the M1 site is usually thought to be preferred by smaller cations. Since olivine is a solid solution of magnesium and iron, we chose 15 bulk structures in which the  $Fe : Mg$  equal 2 : 6, 4 : 4 and 6 : 2 in bulk unit cells which the iron contents are 25%, 50% and 75% respectively to cover the iron composition range from low to high. In each composition, the iron atoms are placed in different metal cation sites to build the different bulk structures. We named the structure with the cations in the M1 site(Figure. 2 and Figure. 5).

The catalytic activity of olivines in biomass gasification was proposed to be due to the presence of iron atoms on the surface and tested in several experimental studies[9]. We construct a series iron contained olivine surface slabs based on two types (Figure. 5) most possible exposed surface terminations one type with  $M2$  site exposed and another type with  $M1$  site exposed based on our previous studies[22]. The  $M2$  exposed type of surfaces are relatively flatter than the  $M1$  exposed ones, no matter whether the iron atoms are on the top or not. We only choose the low iron content (2 Fe atom/slab and 4 Fe atom/slab of metal atoms) in our slab models, so we can consider iron as an impurity so the relative stability of surfaces will not differ much from the forsterite slabs. This strategy fits the fact that natural olivine usually has relatively low iron content. Therefore, the slab model we chose is good enough to represent the most likely stable surfaces. To minimize the effect of the periodic boundary conditions, a 30 Åthick vacuum space is added on the top of the surface slab models. All the atoms in the slabs are relaxed prior to energy calculation.

## B. Computation methods

The DFT calculations make use of the Perdew-Burke-Ernzerhof (PBE) approximation to the exchange-correlation functional with a 700 eV kinetic energy cutoff in the plane wave basis set. The projector augmented wave method is used to describe the effect of the inner electrons. Monkhorst-Pack k-point mesh was used in the optimization of bulk crystal phase ( $8 \times 8 \times 8$ ) and surface slabs ( $8 \times 8 \times 1$ ). The ground-state atomic geometries of the bulk and surface are obtained by minimizing the force on each atom to below 0.01 eV/Å. The Vienna Ab initio simulation package (VASP)[23, 24] is used to perform the DFT calculation. For minerals containing iron, the 3d orbitals of iron can make up by two sets of orbitals  $t_{2g}$  and  $e_g$ .  $Fe^{2+}$  can have high spin and low spin state, high-spin is the quintet ( $S = 2, 2S + 1 = 5$ ) which the difference of electrons spin up and spin down is 4 per Fe atom, while low-spin is the singlet ( $S = 0, 2S + 1 = 1$ ) which the difference of electron spin up and spin down is 0 per Fe atom. So spin polarization should be considered in the calculation due to the possible spin transition in many iron containing mantle minerals[25, 26]. All the calculation are run as spin-polarized and the ground state of the bulk system are tested with both DFT+U method with an effective U value (U=4.5 eV, J=0.9 eV) adopted from previous works[27–29] and strongly constrained appropriately normed (SCAN) meta-GGA[30]. As the SCAN functional sometime has some difficulties in geometry optimization, we used the optimized results with PBE as the initial structure of SCAN and PBE+U optimization calculation. The distribution of the Fe atom will not always be symmetry in the slab models. A dipole correction is applied in the slab calculation.

## C. Thermodynamics

In most studies, ground state total energies from DFT calculations were directly used for estimating the stability of different structures. But many experiments reported the ordering distribution of cations can be affected by temperature. Iron bearing olivine will have an order-disorder transition at a certain temperature. Unfortunately, the transition temperature also didn't reach an agreement in different experiments. By evaluating the Gibbs free energy, the temperature and composition differences can be taken into account in the analysis of structure stability. The Gibbs free energy  $G$  can be calculated as

$$G(T) = E_{DFT} + F^{vib}(T) - TS^{conf} + pV \quad (2)$$

$E_{DFT}$  is the ground state total energy from the DFT calculation,  $F^{vib}(T)$  is the vibrational energy contribution,  $S^{conf}$  is the configurational ("mixing") entropy. The volume per unit crystal cell is  $299.12 \text{ \AA}^3$ , from some experiment results the volume variation under 15GPa is small,

which makes the  $pV$  term can be at the common error level of DFT calculation. On the other hand, the energy difference ( $\Delta G$ ) of different structures is important in the comparison, the volume difference of the structures can be extremely small when the composition is the same, so we can neglect the  $pV$  term.

$$\Delta G(T) = \Delta E + \Delta F^{vib}(T) - T\Delta S^{conf} \quad (3)$$

We considered the configurational entropy ( $S^{conf}$ ) of the system explicitly as follow due to the different distribution of iron atoms in the lattice.

$$S^{conf} = -k_B \sum_j (m_j \sum_i X_{ij} \ln X_{ij}) \quad (4)$$

where  $m_j$  is the total number of atoms in the  $j^{th}$  crystallographic and  $X_{i,j}$  is the mole fraction of the  $i^{th}$  atom in the  $j^{th}$  site.

The vibrational contribution term  $F^{vib}(T)$  can be expressed using phonon density of states as follow

$$F^{vib}(T) = \frac{1}{2} \sum_{qj} h\omega_{qj} + k_B T \sum_{qj} \ln[1 - e^{(-h\omega_{qj})/k_B T}] \quad (5)$$

where  $q$  is the wave vector,  $j$  is the band index, and  $\omega_{qj}$  is the phonon frequency of the phonon mode labelled by set  $q, j$ . The phonon calculations are conducted using density functional perturbation theory (DFPT) as implemented in the VASP/Phonopy software [31].

Based on experience in a study of diffusion in solid system[32], we used a model based on the energetics of swapping Mg and Fe atoms in inequivalent sites of the system which allows us to predict the probability of Fe diffusion to certain site. In this case, the metal sites can be occupied either by Mg atom or Fe atom. The probability of a site is occupied by Fe can be estimated by a Fermi-Dirac distribution model.

$$n(\Delta E, \Delta\mu, T) = \frac{1}{e^{(\Delta E - \Delta\mu)/k_B T} + 1} \quad (6)$$

which  $\Delta E$  is the swapping energy of the Mg and Fe atoms,  $\Delta\mu$  is a relative chemical potential for replacing an Mg atom with a Fe atom. Since the  $\Delta\mu$  can be approximately estimated from the free energy difference of bulk system with one more Fe atom replacing the Mg atom to the reference system. But the Gibbs free energy of this approach is composition related, one atom change in a small system can lead to large composition change. To overcome this, we calculated  $\Delta\mu$  for a series of supercells that have a similar composition ratio as our surface slabs.

### III. RESULTS AND DISCUSSION

#### A. Structure optimization

We have performed structural optimization for bulk systems of 3 different chemical compositions in order to obtain the most stable configuration as the initial crystal structures adopted from the experiment result have a different chemical composition. With the Fe atoms added, the energy surfaces became rougher than the forsterite (pure magnesium structure) system, which takes some effort to reach convergence in structure optimization.

The optimized results of the primitive cell of olivine with different composition in orthorhombic structures are shown in Table I. There is no experimental data available with the exact same chemical composition for some structures. Only the Fo50 structure can be directly compared to the experimental result. However, by comparing the experimental results [33–35] of pure end members forsterite, fayalite and Fo50, the error in our results should be less than 5%.

As shown in Table. IV, no matter in the forsterite or fayalite structure, the M1 octahedra is slightly smaller than the M2 octahedra. So some previous studies claim the slight preference of the Fe atom to the M1 site is because the ion radius of  $Fe^{2+}$  is smaller than  $Mg^{2+}$ [36]. However, the ion radius is not the same between two spin states. The  $Fe^{2+}$  radius is smaller than  $Mg^{2+}$  only when the  $Fe^{2+}$  is in its low spin state[37]. Usually, the low spin state is the dominant state under high pressure when the orbital splitting is smaller. Theoretic research[38] predicted the spin transition from high spin to low spin of the Fayalite will happen around 15GPa, and experimental observation[39] suggested this spin transition would happen under higher pressure, between 40 and 50 GPa. We evaluated the electron-spin multiplicity by fixing the difference of electron spin up and spin down in the VASP calculation. Our calculation result for bulk is in Table. V shows high spin states always have lower energy than low spin. Our calculation result fits the experiment fact that the  $Fe^{2+}$  is in the high spin state where natural olivine exists. The ion radius of high spin  $Fe^{2+}$  is bigger, so the octahedra need larger space. Correspondingly in the Table. IV, we found the octahedra will be expanded when iron is in the site, regardless of M1 or M2 site. In all the conditions,  $SiO$  tetrahedra is slightly larger than the tetrahedra in forsterite (pure magnesium) or fayalite (pure iron), but when the composition is fixed the tetrahedra will keep about the same size.

The slab results in Table. VI show high spin states  $Fe^{2+}$  also have the lower energies in surface slabs. The  $Fe^{2+}$  should occupy larger space than  $Mg^{2+}$ . However, the surface geometry feature breaks some polyhedra in the surface slab. Grid-based Bader analysis[40] (Table II) gave us the atomic volume of the cations purely based on the electronic charge density. We find the Fe atoms always have a larger volume than Mg no matter inside the bulk or exposed on the surface. The Fe atoms in-

volvement did not change the charge distribution of the slab. Similar to our previous result with forsterite surface, the charge differences of the same atom is small in the slabs. But the oxygen atoms are divided into groups by the cation it associated with.

#### B. Ground state preference: Total-energy calculations

To test the calculation level of our study, we calculated the total energies of Fo50 ( $Mg : Fe = 4 : 4$ ) olivines within PBE, PBE+U and SCAN three different functionals (Table. III). We find the energy of the system increases with the swapping of the Fe atoms from M1 site to M2 site. In PBE calculation, the energy difference between all  $Fe^{2+}$  in the M1 and all  $Fe^{2+}$  in the M2 is  $0.475eV$  and the atom difference between is 4 atoms. Some previous studies used GGA+U to calculate the elasticity of fayalite and hydrous fayalite due to the 3d electrons of Fe atom[29]. In VASP the U value is set by two constants U and J. We simply adopted the U value from some previous studies[8, 27, 29] to test the energies of the structures in our study since different studies used the same U and J value. The results we get from PBE+U calculation did not show enough difference whether the Fe atoms are in M1 or M2 site. At same time we used the SCAN which recently developed meta-GGA functional shows good performance on calculating system with transition metal atoms. We get a similar energy difference ( $0.314eV$ ) as PBE calculation in the SCAN calculation. The energies in SCAN calculation show the same trend as the PBE result, all the Fe atom in the M1 site has the lowest energy among comparing structures. And both the energies from PBE and SCAN results increases with the more iron atom moved to M1 site from M2 site and it grows linearly with the atom move which indicated Fe atoms prefers the M1 site although the  $Fe^{2+}$  cations in high spin state have the larger ion radius than  $Mg^{2+}$ . The adopted U value in our study is not good enough to find out the energy difference of the distribution variation of the olivine system. The U value should be adjusted when the composition changes. From the results above, we find the PBE is good enough to find out the energy preference of different configurations, and also the structures we investigate are not the same in chemical composition. So we used PBE for the following calculation.

A similar energy characteristic shows in both the high and low Fe concentrations conditions. The more Fe atom in the M1 site the lower energy the system have. When the Fe concentration drops to  $Mg : Fe = 6 : 2$  (Fo75), the highest difference of Fe in M1 site and M2 site is 2 Fe atoms per unit-cell, and the the energy difference is  $0.212eV$ . In Fo25, the structures have higher Fe concentration ( $Mg : Fe = 2 : 6$ ). The largest Fe atom difference between structures is also 2 atoms per unit-cell which have a energy difference of  $0.492eV$ . We find the

energy difference per atom keeps about the same from Fo75 to Fo50 and increases from Fo50 to Fo25 with the Fe concentration raise. This indicates the more Fe in the system the higher energy preference to move the Fe atom from M2 to M1 sites.

### C. Entropy effect

Recently study[41] on Fe containing carbonate claimed the magnetic entropy caused by the distribution of Fe atoms with different spin states can be important in mineral stabilization in the mantle. Since the natural occurrence of olivine is mainly no more than 14GPa, far lower than the experiment observed spin transition pressure, we did not consider the systems under higher pressure. As described before, high spin states always have a lower energy in our calculation, which means all the Fe atoms are all in the same spin state, so the magnetic entropy could be neglected in our research.

Since two different kinds of cations are involved in the system, the structures can be categorised into two groups: ordered group and mixed group. For example in Figure. 2, Fo50 Fe0Mg4 and Fe4Mg0 are the ordered structures which have the lowest and highest  $k_D$  value respectively. The  $k_D$  value of Fe4Mg0 in Fo50 which has the fully mixed distribution of Mg and  $Fe^{2+}$  cations is 1. These cation distributions cause the 0K total energy difference due to the preference of  $Fe^{2+}$ . The more  $Fe^{2+}$  distributed in the M1 site, the lower energy the structure has. The ordered group have the lowest and highest energy and the mixed group lays in between the two ordered structures. However, these two types of cations distributed into different sites will cause the mixing entropy. The mixing entropy is much less than  $-0.01eV/K$  and the free energy contribution is just meV level when at the low temperature. Pressure effects on the cation distribution order-disorder of main minerals was reviewed by Hazen and Navrotsky[42].  $\Delta V_{dis} = V_{disordered} - V_{ordered}$  derived from Akamatsu et al.[15] experiment is only  $\Delta V_{dis} = 0.24cm^3/mol = 1.6 \times 10^{-3}\text{\AA}^3/unitcell$ , so we can neglect the pressure effect of the mixing energy contribution in our pressure range. When the temperature raise to 1500K, the maximum difference of free energy contribution of mixing entropy between orderer and disordered structure is about  $0.79eV$  which is about the similar order of magnitude of the ground total energy difference caused by the  $Fe^{2+}$  distribution. Therefore, the mixing entropy should be considered in the free energy when evaluating the temperature effect of the cation distribution. Vibrational entropy is also believed to play an important role in free energy contribution at high temperatures. As we can find in the Figure. 6, the vibrational entropy only shrunken the energy gaps of the mixed group structures and the M1 ordered structure and no energy crossover is found under 1600K in our study. The mixing entropy only can cause some energy crossovers in the temperature range.

As we expected, with both mixing and vibrational entropy considered in the Gibbs free energy evaluation, we can find the fully ordered structure  $Fe0Mg4$  is the most stable structure at low temperature and the most disordered structure  $Fe2Mg2$  is the most stable structure at the high temperature. Except the ordered M2 structure  $Fe4Mg0$ , the energy difference is small among the rest structures. The large energy gap between M2 ordered structure and the rest also indicates it is highly difficult to distribute  $Fe^{2+}$  into M2 site even at high temperatures. In experiment, it is quite difficult to precisely know one site is taken over by  $Fe^{2+}$  or  $Mg$  [43], so  $k_D$  value became their important indicator to know the site preference. In Fo50 by Redfern et al.[34] find out the  $k_D = 1$  at around 898K. We can find a similar energy crossover of the most disorder structure  $Fe2Mg2$  which  $k_D = 1$  in Fo50 at 850K and became the most stable one among 5 possible structures. This crossover also means the site preference of  $Fe^{2+}$  to M1 will disappear above this temperature, unlike many experiment research claimed the preference will increase continuously with rising temperature[44, 45]. Figure. 7 shows this crossover temperature moves to lower temperature when the chemical composition is more  $Mg$  rich and  $Fe$  poor, and the  $k_D$  value in the different chemical systems is also not the same.

### D. Surface Exposure

Although olivine was used as a catalyst in many chemical reactions, very limited research was done on the surface cation distribution. In the surface slab, the surface exposure of a site can be quite critical to the cation distribution due to the unique geometric characteristic of the surface. The atoms exposed on the surface will gain extra space from the outside which can be seen from the Figure. 4. Atoms near the surface have larger displacements than the atom inside the slab during the relaxation. Similar to what we found in the bulk system result, the  $Fe^{2+}$  in high spin state also have lower energy than in the low spin state on the surface site. Previous study on Fo75 olivine surface with B3LYP functional showed the quintet state is the lowest energy state[20] when the  $Fe^{2+}$  occupied the surface site. But we did not find the  $Fe^{2+}$  have larger splitting of  $3d$  orbitals under saturated environments inside the slab their study reported[20]. In bulk system the  $Fe^{2+}$  is always in saturated environment and the spin transition from high spin to low spin only happens under high pressure. In our result, the  $Fe^{2+}$  in the slab showed similar behaviour as it in the bulk system, quintet state always has the lowest energy no matter it is inside the slab or exposed on the surface.

A preference to M1 site over than M2 site of  $Fe^{2+}$  can be observed if all  $Fe^{2+}$  atom is inside the slab. The relative position of  $Fe^{2+}$ s also affect the energies. Structures with two  $Fe^{2+}$  cations next to each other have lower energy than the structures two  $Fe^{2+}$  separated by  $Mg^{2+}$ .

However, the metal site exposed on the surface can lead an obvious preference of  $Fe^{2+}$  regardless the site is M1 or M2 site. But the energy needed to swap  $Fe^{2+}$  to the surface is not the same because the different cleavage energy to form different surface terminations. As we mentioned before, the octahedra of the metal site would be enlarged when  $Fe^{2+}$  occupied the site. Obviously, the on surface exposed site can easily provide larger space than any other metal site inside the slab for the  $Fe^{2+}$  because of the unsaturated geometric nature. The energy difference of surface exposure cation site and any interior cation site will highly possible become a driving force for  $Fe^{2+}$  diffusion from any cation site to the surface.

With the relative chemical potential get from the supercell results, we estimated the occupation probability of Fe atoms move to a particular site after diffusion based on the energetics in Figure 8. We compared the probability of moving  $Fe^{2+}$  to M2 site inside the bulk and if the M2 site is on the surface. It is quite clear that  $Fe^{2+}$  shows higher probability move to M2 site if the site is exposed on the surface. This also indicated the surface of the olivine can have a higher Fe concentration than the bulk due to the diffusion of Fe atom and the catalytic ability iron contained olivine shown in many reactions is highly based on the  $Fe^{2+}$  on the surface. A lot of natural olivines have a kind of zoning structure which have a higher Fe concentration on the edge than the center of the crystal. The chemical zoning of the natural olivine was think formed by the sequential magma activity when the olivine growing, but the diffusion of metal ions after the olivine crystallized became more focused and became an emerging tool to understand the volcano's eruptive past[46]. Since the  $Fe^{2+}$ 's trend to diffuse to the surface which behave the same pattern as the experiment observed in the olivine chemical zoning. Grain boundary effect which is ignored in the past models[47] should be definitely considered in future models of diffusion chronometry.

#### IV. CONCLUSION

We used DFT calculation combined thermodynamics to analyze bulk crystal and surface slab of olivine with different Fe concentrations from iron rich (Fo25) to iron poor (Fo75). The relative stability of olivine crystals and slabs with different  $Fe^{2+}$  cation distribution is estimated based on the Gibbs free energy. Meanwhile, this relative

stability indicated the preference of Fe atom between different metal sites in the olivine crystal structure. We found the high spin state is the most stable spin state of  $Fe^{2+}$  under ambient pressure, which leads a larger ion radius of  $Fe^{2+}$  than  $Mg^{2+}$  in the crystal. This means a larger metal-oxygen octahedron is needed in olivine to put the  $Fe^{2+}$  in. Although the M1 site octahedra is smaller than M2 site in both Mg and Fe endmembers of olivine, the  $Fe^{2+}$  is still energetically preferred M1 site, from both our PBE and SCAN calculations, when Fe is added to the system by enlarging the metal-oxygen octahedra. This is not consistent with previous studies that  $Fe^{2+}$  prefer M1 site because of its smaller size than  $Mg^{2+}$ . The energy contribution of entropies accumulating with the temperature increases, and the vibrational entropy shrink the energy difference of different structures while the mixing entropy fills the energy gap of order and disorder distribution of  $Fe^{2+}$  in the olivine crystal under high temperature at the same time. At the order-disorder energy crossover temperature, the preference to M1 site of  $Fe^{2+}$  will disappear due to these entropy contributions.

Similar to the bulk system, high spin state also is the stable state of  $Fe^{2+}$  in surface slabs. This lead  $Fe^{2+}$  inside the surface slab distribute with the same principle as in the bulk. Once a metal site exposes on the surface will easily provide larger space for the cation because of the geometric character. This feature make surface exposed metal site became more preferable to  $Fe^{2+}$  than any metal site inside the slab no matter M1 or M2 site. This indicates the impurity  $Fe^{2+}$  in olivine can be highly possible on the surface of olivine by diffusion from bulk to the surface driving by the energy preference. Since  $Fe^{2+}$  have a 3d electron orbital, this implication shows Fe atom in the olivine can play a critical role as a catalyst in many geochemical reactions which many are shown in the olivine related reactions.

#### ACKNOWLEDGMENTS

This work was supported by Icelandic Research Fund. MG acknowledge financial support from the Research Council of Norway through its Centres of Excellence scheme, project number 223272 (CEED). The computations were performed on resources provided by the Icelandic High-Performance Computing Centre at the University of Iceland and the Norwegian infrastructure for high-performance computing (NOTUR, Sigma-2, Grants NN9329K and NN2916K).

---

[1] M. Stimpfl, A. M. Walker, M. J. Drake, N. H. de Leeuw, and P. Deymier, An angström-sized window on the origin of water in the inner solar system: Atomistic simulation of adsorption of water on olivine, *Journal of Crystal Growth* **294**, 83 (2006).

[2] M. D'Angelo, S. Cazaux, I. Kamp, W.-F. Thi, and

P. Woitke, Water delivery in the inner solar nebula, *Astronomy & Astrophysics* **622**, A208 (2019).

[3] S. Mahendran, P. Carrez, and P. Cordier, On the glide of [100] dislocation and the origin of 'pencil glide' in  $mg_2sio_4$  olivine, *Philosophical Magazine* **99**, 2751 (2019).

[4] J. Navarro-Ruiz, P. Ugliengo, M. Sodupe, and A. Rimola,

- Does  $\text{Fe}^{2+}$  in olivine-based interstellar grains play any role in the formation of  $\text{H}_2$ ? atomistic insights from dft periodic simulations, *Chemical Communications* **52**, 6873 (2016).
- [5] I. Oueslati, B. Kerkeni, and S. T. Bromley, Trends in the adsorption and reactivity of hydrogen on magnesium silicate nanoclusters, *Physical Chemistry Chemical Physics* **17**, 8951 (2015).
- [6] M. Akaogi, E. Ito, and A. Navrotsky, Olivine-modified spinel-spinel transitions in the system  $\text{Mg}_2\text{SiO}_4\text{-Fe}_2\text{SiO}_4$ : Calorimetric measurements, thermochemical calculation, and geophysical application, *Journal of Geophysical Research: Solid Earth* **94**, 15671 (1989).
- [7] C. R. Bina and B. J. Wood, Olivine-spinel transitions: Experimental and thermodynamic constraints and implications for the nature of the 400-km seismic discontinuity, *Journal of Geophysical Research: Solid Earth* **92**, 4853 (1987).
- [8] P. K. Das, N. Mandal, and A. Arya, Effects of cation ordering on the elastic and electronic properties of mg-fe silicate phases at high pressures, *Journal of Applied Physics* **122**, 225107 (2017).
- [9] H. O. A. Fredriksson, R. J. Lancee, P. C. Thüne, H. J. Veringa, and J. W. Niemantsverdriet, Olivine as tar removal catalyst in biomass gasification: Catalyst dynamics under model conditions, *Applied Catalysis B: Environmental* **130-131**, 168 (2013).
- [10] N. Mandal, K. H. Chakravarty, K. Borah, and S. S. Rai, Is a cation ordering transition of the mg-fe olivine phase in the mantle responsible for the shallow mantle seismic discontinuity beneath the Indian craton?, *Journal of Geophysical Research: Solid Earth* **117**, 10.1029/2012jb009225 (2012).
- [11] N. R. Khisina, E. L. Belokoneva, D. Vasiliev, and M. Siminov, Intracrystalline distribution of Fe and Mg in the structures of three natural olivines, *Dokl. Akad. Nauk SSSR* **276**, 873 (1984).
- [12] N. Aikawa, M. Kumazawa, and M. Tokonami, Temperature dependence of intersite distribution of Mg and Fe in olivine and the associated change of lattice parameters, *Physics and Chemistry of Minerals* **12**, 1 (1985).
- [13] G. Artioli, R. Rinaldi, C. C. Wilson, and P. F. Zanazzi, High-temperature Fe-Mg cation partitioning in olivine: In-situ single-crystal neutron diffraction study, *American Mineralogist* **80**, 197 (1995).
- [14] F. Princivalle, Influence of temperature and composition on Mg-Fe<sup>2+</sup> intracrystalline distribution in olivines, *Mineralogy and Petrology* **43**, 121 (1990).
- [15] T. Akamatsu, M. Kumazawa, N. Aikawa, and H. Takei, Pressure effect on the divalent cation distribution in non-ideal solid solution of forsterite and fayalite, *Physics and Chemistry of Minerals* **19**, 431 (1993).
- [16] W. A. Deer, R. A. Howie, and J. Zussman, *Rock forming minerals. 1A, 1A* (Geological Society, London, 2001).
- [17] M. N. Taran and S. S. Matsyuk, Fe<sup>2+</sup>, Mg-distribution among non-equivalent structural sites m1 and m2 in natural olivines: an optical spectroscopy study, *Physics and Chemistry of Minerals* **40**, 309 (2013).
- [18] R. J. McCarty, A. C. Palke, J. F. Stebbins, and J. S. Hartman, Transition metal cation site preferences in forsterite ( $\text{Mg}_2\text{SiO}_4$ ) determined from paramagnetically shifted NMR resonances, *American Mineralogist* **100**, 1265 (2015).
- [19] S. Chatterjee, S. Sengupta, T. Saha-Dasgupta, K. Chatterjee, and N. Mandal, Site preference of Fe atoms in  $\text{FeMgSiO}_4$  and  $\text{FeMg}(\text{SiO}_3)_2$  studied by density functional calculations, *Physical Review B* **79**, 115103 (2009).
- [20] J. Navarro-Ruiz, P. Ugliengo, A. Rimola, and M. Sodupe, B3lyp periodic study of the physicochemical properties of the nonpolar (010) Mg-pure and Fe-containing olivine surfaces, *The Journal of Physical Chemistry A* **118**, 5866 (2014).
- [21] J. R. Smyth, High temperature crystal chemistry of fayalite, *American Mineralogist* **60**, 1092 (1975).
- [22] M. Geng and H. Jónsson, Density functional theory calculations and thermodynamic analysis of the forsterite  $\text{Mg}_2\text{SiO}_4(010)$  surface, *The Journal of Physical Chemistry C* **123**, 464 (2019).
- [23] G. Kresse and J. Furthmüller, Efficient iterative schemes for ab initio total-energy calculations using a plane-wave basis set, *Physical Review B* **54**, 11169 (1996).
- [24] G. Kresse and D. Joubert, From ultrasoft pseudopotentials to the projector augmented-wave method, *Physical Review B* **59**, 1758 (1999).
- [25] T. Tsuchiya, R. M. Wentzcovitch, C. R. S. da Silva, and S. de Gironcoli, Spin transition in magnesiowüstite in earth's lower mantle, *Physical Review Letters* **96**, 198501 (2006).
- [26] E. Holmström and L. Stixrude, Spin crossover in ferropericlase from first-principles molecular dynamics, *Physical Review Letters* **114**, 117202 (2015).
- [27] L. Xiao, X. Li, and X. Yang, Electronic and optical properties of  $\text{Fe}_2\text{SiO}_4$  under pressure effect: ab initio study, *The European Physical Journal B* **91**, 85 (2018).
- [28] X. Jiang and G. Y. Guo, First-principles studies of the electronic structure and magnetism in fayalites:  $\text{M}_2\text{SiO}_4$  (m=Fe and Co), *Journal of Magnetism and Magnetic Materials* **282**, 287 (2004).
- [29] C.-Y. Zhang, X.-B. Wang, X.-F. Zhao, X.-R. Chen, Y. Yu, and X.-F. Tian, First-principles calculations of structure and elasticity of hydrous fayalite under high pressure, *Chinese Physics B* **26**, 126103 (2017).
- [30] J. Sun, R. C. Remsing, Y. Zhang, Z. Sun, A. Ruzsinszky, H. Peng, Z. Yang, A. Paul, U. Waghmare, X. Wu, M. L. Klein, and J. P. Perdew, Accurate first-principles structures and energies of diversely bonded systems from an efficient density functional, *Nature Chemistry* **8**, 831 (2016).
- [31] A. Togo and I. Tanaka, First principles phonon calculations in materials science, *Scripta Materialia* **108**, 1 (2015).
- [32] B. P. Uberuaga, M. Leskovaar, A. P. Smith, H. Jónsson, and M. Olmstead, Diffusion of Ge below the Si(100) surface: Theory and experiment, *Physical Review Letters* **84**, 2441 (2000).
- [33] A. Kirfel, T. Lippmann, P. Blaha, K. Schwarz, D. F. Cox, K. M. Rosso, and G. V. Gibbs, Electron density distribution and bond critical point properties for forsterite,  $\text{Mg}_2\text{SiO}_4$ , determined with synchrotron single crystal x-ray diffraction data, *Physics and Chemistry of Minerals* **32**, 301 (2005).
- [34] S. A. T. Redfern, G. Artioli, R. Rinaldi, C. M. B. Henderson, K. S. Knight, and B. J. Wood, Octahedral cation ordering in olivine at high temperature. ii: an in situ neutron powder diffraction study on synthetic  $\text{MgFeSiO}_4$  (fa50), *Physics and Chemistry of Minerals* **27**, 630 (2000).
- [35] Y. Kudoh and H. Takeda, Single crystal x-ray diffraction study on the bond compressibility of fayalite,  $\text{Fe}_2\text{SiO}_4$  and rutile,  $\text{TiO}_2$  under high pressure, *Physica B+C* **139-140**,

- 333 (1986).
- [36] G. E. Brown, Olivines and silicate spinels, *Reviews in Mineralogy and Geochemistry* **5**, 275 (1980).
- [37] R. Shannon, Revised effective ionic radii and systematic studies of interatomic distances in halides and chalcogenides, *Acta Crystallographica Section A* **32**, 751 (1976).
- [38] M. Núñez Valdez, K. Umemoto, and R. M. Wentzcovitch, Fundamentals of elasticity of  $(\text{mg}_{1-x}, \text{fe}_x)_2\text{siO}_4$  olivine, *Geophysical Research Letters* **37**, 2098 (2010).
- [39] J. Rouquette, I. Kantor, C. A. McCammon, V. Dmitriev, and L. S. Dubrovinsky, High-pressure studies of  $(\text{mg}_{0.9}\text{fe}_{0.1})_2\text{siO}_4$  olivine using raman spectroscopy, x-ray diffraction, and mössbauer spectroscopy, *Inorganic Chemistry* **47**, 2668 (2008).
- [40] G. Henkelman, A. Arnaldsson, and H. Jónsson, A fast and robust algorithm for bader decomposition of charge density, *Computational Materials Science* **36**, 354 (2006).
- [41] Z. Li and S. Stackhouse, Iron-rich carbonates stabilized by magnetic entropy at lower mantle conditions, *Earth and Planetary Science Letters*, 115959 (2019).
- [42] R. M. Hazen and A. Navrotsky, Effects of pressure on order-disorder reactions, *American Mineralogist* **81**, 1021 (1996).
- [43] Z. Y. Wu, A. Mottana, A. Marcelli, E. Paris, G. Giuli, and G. Cibir, X-ray absorption near-edge structure at the mg and fe  $k$  edges in olivine minerals, *Physical Review B* **69**, 104106 (2004).
- [44] M. Morozov, C. Brinkmann, W. Lottermoser, G. Tippelt, G. Amthauer, and H. Kroll, Octahedral cation partitioning in  $\text{mg,fe}^{2+}$ -olivine. mössbauer spectroscopic study of synthetic  $(\text{mg}_{0.5}\text{fe}_{0.5}^{2+})_2\text{siO}_4$  (fa50), *European Journal of Mineralogy* **17**, 495 (2005).
- [45] M. N. Taran and M. Koch-Müller, Octahedral cation ordering in  $\text{mg, fe}^{2+}$ -olivine: an optical absorption spectroscopic study, *Physics and Chemistry of Minerals* **33**, 511 (2006).
- [46] J. Rosen, Crystal clocks, *Science* **354**, 822 (2016).
- [47] F. Costa, T. Shea, and T. Ubide, Diffusion chronometry and the timescales of magmatic processes, *Nature Reviews Earth & Environment* **1**, 201 (2020).
- [48] T. Qin, R. M. Wentzcovitch, K. Umemoto, M. M. Hirschmann, and D. L. Kohlstedt, Ab initio study of water speciation in forsterite: Importance of the entropic effect, *American Mineralogist* **103**, 692 (2018).
- [49] S. Chatterjee and T. Saha-Dasgupta, First-principles simulations of structural, electronic, and magnetic properties of vacancy-bearing fe silicates, *Physical Review B* **81**, 155105 (2010).
- [50] J. Shi, S. Ganschow, D. Klimm, K. Simon, R. Bertram, and K.-D. Becker, Octahedral cation exchange in  $(\text{co}_{0.21}\text{mg}_{0.79})_2\text{siO}_4$  olivine at high temperatures: Kinetics, point defect chemistry, and cation diffusion, *The Journal of Physical Chemistry C* **113**, 6267 (2009).
- [51] G. Ottonello, F. Princivalle, and A. Della Giusta, Temperature, composition, and  $\text{fo}_2$  effects on intersite distribution of mg and  $\text{fe}^{2+}$  in olivines, *Physics and Chemistry of Minerals* **17**, 301 (1990).
- [52] R. Rinaldi, G. Artioli, C. C. Wilson, and G. McIntyre, Octahedral cation ordering in olivine at high temperature. i: in situ neutron single-crystal diffraction studies on natural mantle olivines (fa12 and fa10), *Physics and Chemistry of Minerals* **27**, 623 (2000).
- [53] M. Cococcioni, A. Dal Corso, and S. de Gironcoli, Structural, electronic, and magnetic properties of  $\text{fe}_2\text{siO}_4$  fayalite: Comparison of lda and gga results, *Physical Review B* **67**, 094106 (2003).
- [54] J. Heath, H. Chen, and M. S. Islam,  $\text{MgFeSiO}_4$  as a potential cathode material for magnesium batteries: ion diffusion rates and voltage trends, *Journal of Materials Chemistry A* **5**, 13161 (2017).
- [55] M. Kadziolka-Gawel, M. Dulski, L. Kalinowski, and M. Wojtyniak, The effect of gamma irradiation on the structural properties of olivine, *Journal of Radioanalytical and Nuclear Chemistry* **317**, 261 (2018).
- [56] M. N. Taran, M. Núñez Valdez, I. Efthimiopoulos, J. Müller, H. J. Reichmann, M. Wilke, and M. Koch-Müller, Spectroscopic and ab initio studies of the pressure-induced  $\text{fe}^{2+}$  high-spin-to-low-spin electronic transition in natural triphylite-lithiophilite, *Physics and Chemistry of Minerals* **46**, 245 (2019).
- [57] C. Ling, D. Banerjee, W. Song, M. Zhang, and M. Matsui, First-principles study of the magnesianation of olivines: redox reaction mechanism, electrochemical and thermodynamic properties, *Journal of Materials Chemistry* **22**, 13517 (2012).
- [58] I. Kushiro and B. O. Mysen, A possible effect of melt structure on the  $\text{mg-fe}^{2+}$  partitioning between olivine and melt, *Geochimica et Cosmochimica Acta* **66**, 2267 (2002).
- [59] I. Kushiro and M. J. Walter, Mg-fe partitioning between olivine and mafic-ultramafic melts, *Geophysical Research Letters* **25**, 2337 (1998).



TABLE I. Experimental and Calculated Values for Cell Parameters of Bulk Forsterite (in Å)

Lattice Constant	Experiment			This work		
	Forsterite [33]	Fo50 [34]	Fayalite [35]	Fo75	Fo50	Fo25
a	4.76	4.81	4.82	4.83	4.88	4.88
b	10.20	10.38	10.49	10.50	10.51	10.51
c	5.98	6.06	6.10	6.14	6.16	6.16

TABLE II. Bader analysis of the surface slabs. The bader volume is in Å<sup>3</sup> and the bader charge of different surface slabs.

Surface Slab	Bader Volume (Charge)								Surface Slab	Bader Volume (Charge)							
	Top				Mid					Top				Mid			
	Fe		Mg		Fe		Mg			Fe		Mg		Fe		Mg	
	M1	M2	M1	M2	M1	M2	M1	M2		M2	Mg	M1	M2	M1	M2		
M2 termination ( 2 Fe Atoms )	Top	159.6 (1.22)		106.8 (1.67)		4.9 (1.68) 5.3 (1.70)				TwoTop	162.3 (1.23)		4.9 (1.68) 5.3 (1.70)				
	Sub			92.8 (1.67)		10.8 (1.32)		4.9 (1.68) 5.2 (1.70)		Top-Sub	90.1 (1.14) 110.3 (1.67)		11.1 (1.31) 4.9 (1.68) 5.3 (1.70)				
	Sub-II			93.0 (1.66)		10.8 (1.32)		4.9 (1.68) 5.2 (1.70)		Top-Sub-II	125.7 (1.17) 104.6 (1.67)		10.9 (1.33) 4.9 (1.68) 5.3 (1.70)				
	Mid			94.8 (1.66)		10.9 (1.38)		4.9 (1.68) 5.4 (1.70)		Top-Mid	157.2 (1.22) 108.4 (1.67) 10.9 (1.39)		4.9 (1.68) 5.2 (1.70)				
	Mid-II			93.4 (1.64)		11.0 (1.38)		4.9 (1.68) 5.2 (1.70)		Top-Mid-II	157.7 (1.21) 106.3 (1.67) 10.8 (1.38)		4.9 (1.68) 5.3 (1.70)				
M1 termination ( 2 Fe Atoms )	Top	69.0 (1.15)		9.1 (1.65)		4.9 (1.68) 5.3 (1.70)				M2 termination ( 4 Fe Atoms )	158.1 (1.22)		102.8 (1.67) 10.9 (1.39)		4.9 (1.68) 5.2 (1.70)		
	Sub			8.7 (1.65)		11.2 (1.35)		4.9 (1.68) 5.4 (1.70)		Sub	88.4 (1.67) 10.7 (1.32)		4.9 (1.68) 5.2 (1.70)				
	Sub-II			8.8 (1.65)		11.2 (1.35)		4.9 (1.68) 5.4 (1.70)		Sub-II	89.2 (1.67) 10.8 (1.32)		4.9 (1.68) 5.3 (1.70)				
	Mid			9.3 (1.65)		10.6 (1.33)		5.0 (1.68) 5.4 (1.70)		Sub-III	87.9 (1.67) 10.8 (1.32)		4.9 (1.68) 5.3 (1.70)				
	Mid-II			9.1 (1.65)		10.3 (1.31)		5.0 (1.68) 5.4 (1.70)		Mid	91.6 (1.67)		11.0 (1.38) 4.9 (1.68)				

TABLE III. Total energy of  $FeMgSiO_4$  (Fe:Mg=4:4) in 0K with different functionals ( $\Delta E = E_{Fe0Mg4} - E$ )

	Fe0Mg4		Fe1Mg3		Fe2Mg2		Fe3Mg1		Fe4Mg0	
	Total Energy(E)	$\Delta E$	Total Energy(E)	$\Delta E$	Total Energy(E)	$\Delta E$	Total Energy(E)	$\Delta E$	Total Energy(E)	$\Delta E$
PBE	-193.195	0.00	-193.250	0.055	-193.326	0.131	-193.455	0.260	-193.669	0.475
SCAN	-300.161	0.00	-300.402	0.241	-300.420	0.259	-300.417	0.256	-300.475	0.314
PBE-U	-188.579	0.00	-189.960	1.381	-189.963	1.384	-189.944	1.365	-189.955	1.376

TABLE IV. Polyhedron volume in Fo50, Forsterite and Fayalite (Å<sup>3</sup>). The Fe atoms form larger octahedra than Mg atoms no matter in M1 or M2 site. SiO tetrahedra keep a similar size.

		Fe0Mg4	Fe1Mg3	Fe2Mg2	Fe3Mg1	Fe4Mg0	Forsterite	Fayalite
M1	Fe		13.45	13.50	13.47	13.58		12.66
	Octahedra	Mg	12.63	13.34	12.70	12.79	11.89	
M2	Fe	14.03	13.99	13.94	13.79			13.18
	Octahedra	Mg		12.64	13.26	13.08	13.11	12.48
SiO tetrahedra		2.32	2.32	2.32	2.32	2.34	2.28	2.20

TABLE V. Relative Energies of bulk structures in high spin and low spin (eV), Reference value is the high spin total energy of least Fe in the M1 site structure in the table for each chemical composition.

Fe:Mg = 2:6 Fo75	Fe0Mg4		Fe0Mg4-II		Fe1Mg3		Fe2Mg2		Fe2Mg2-II	
	High Spin	Low Spin	High Spin	Low Spin	High Spin	Low Spin	High Spin	Low Spin	High Spin	Low Spin
	0.000	1.949	-0.019	2.069	-0.065	2.439	-0.128	2.909	-0.211	2.751
Fe:Mg = 4:4 Fo50	Fe0Mg4		Fe1Mg3		Fe2Mg2		Fe3Mg1		Fe4Mg0	
	High Spin	Low Spin	High Spin	Low Spin	High Spin	Low Spin	High Spin	Low Spin	High Spin	Low Spin
	0.000	5.904	-0.055	5.529	-0.131	2.913	-0.260	4.805	-0.474	4.407
Fe:Mg = 6:2 Fo25	Fe2Mg2		Fe2Mg2-II		Fe3Mg1		Fe4Mg0		Fe4Mg0-II	
	High Spin	Low Spin	High Spin	Low Spin	High Spin	Low Spin	High Spin	Low Spin	High Spin	Low Spin
	0.000	8.048	0.114	8.288	-0.106	7.610	-0.291	7.337	-0.378	7.234

TABLE VI. Relative Total Energies of surface slabs in high spin and low spin state (eV), Reference value is the high spin total energy of first structure in the table for each chemical composition.

	Fe atoms=	Mid		Mid-II		Sub-II		Sub		Top	
		High Spin	Low Spin	High Spin	Low Spin	High Spin	Low Spin	High Spin	Low Spin	High Spin	Low Spin
M2 termination Slabs	2	0.000	2.972	-0.026	2.866	-0.143	1.887	-0.143	1.880	-1.749	1.562
		TwoTop		Top-Sub		Top-Sub-II		Top-Mid		Top-Mid-II	
	4	0.000	-0.026	1.135	6.503	1.308	1.146	1.616	4.760	1.629	1.623
		Sub		Sub-II		Sub-III		Top-Mid-III		Mid	
		High Spin	Low Spin	High Spin	Low Spin	High Spin	Low Spin	High Spin	Low Spin	High Spin	Low Spin
		3.105	5.124	3.042	7.225	3.041	7.173	1.597	7.738	3.313	8.846
M1 termination Slabs	2	Mid		Mid-II		Sub-II		Sub		Top	
		High Spin	Low Spin	High Spin	Low Spin	High Spin	Low Spin	High Spin	Low Spin	High Spin	Low Spin
	0.000	1.994	-0.195	2.026	-0.088	-0.088	-0.088	3.009	-1.789	1.454	

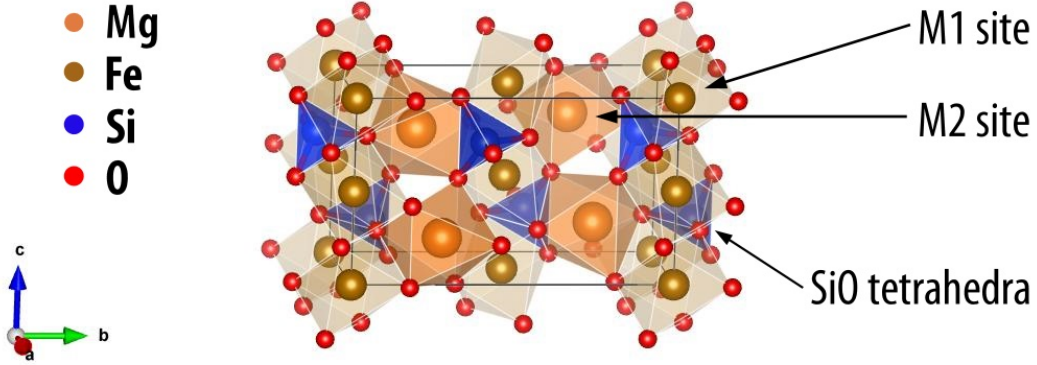


FIG. 1. Structure of olivines crystal (Fo50 as an example) M1 and M2 site are two type of metal cation site, both of these sites with the oxygen around formed two types of octahedra. Silicon and oxygen atoms formed tetrahedra.

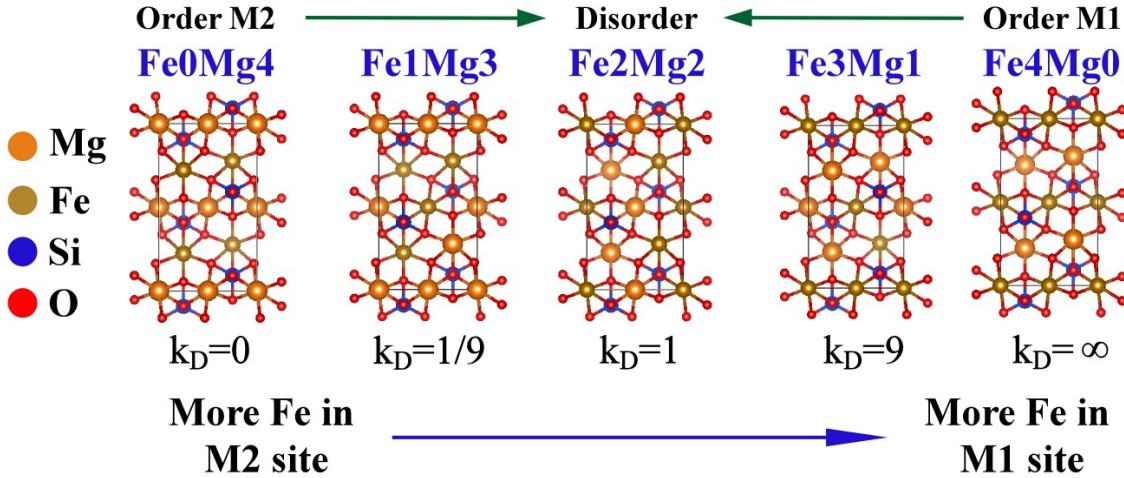


FIG. 2. Side view of Fo50 structures (Mg:Fe = 4:4). The structure is named by the metal atom number in M1 sites.  $k_D$  is the distribution coefficient.  $k_D = 1$  represent a fully mixed structure. The larger  $k_D$  the more Fe atom distributed in the M1 site.

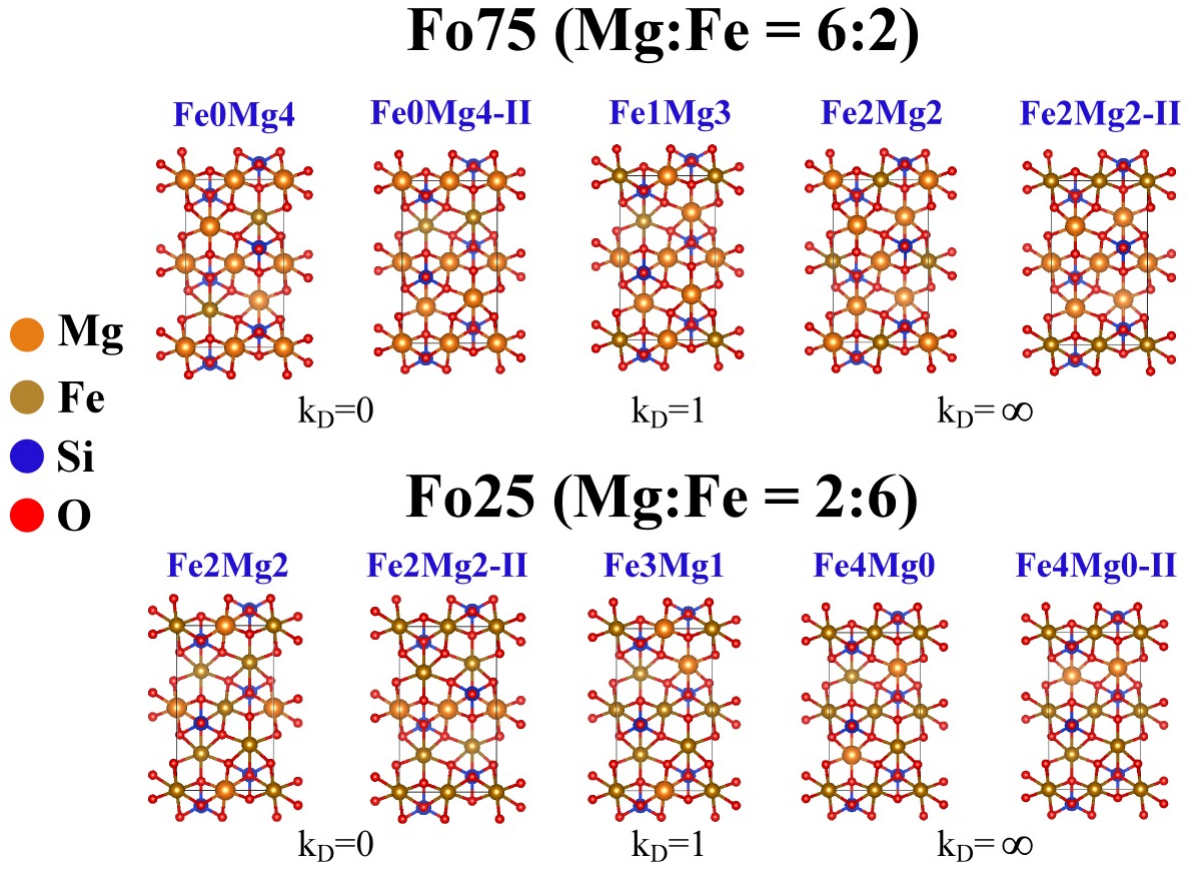


FIG. 3. Structures of the  $(Mg_xFe_{2-x})SiO_4$  with different Fe distribution in iron rich(Fo25) and iron poor(Fo75). The structure is named by the metal atom number in M1 sites.  $k_D$  is the distribution coefficient. The  $k_D$  value shift with the structure chemical composition.

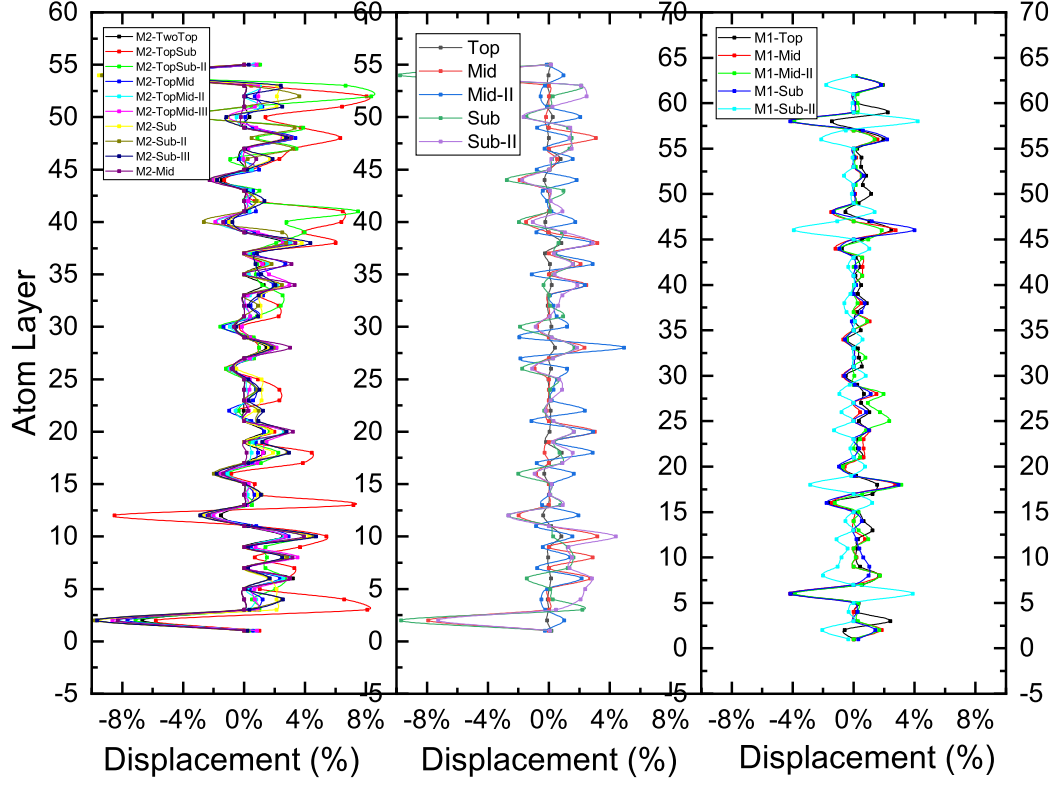


FIG. 4. Atom displacements between origin cleaved slab and relaxed slabs grouped by the different surface termination and Fe concentration. The displacement  $d = \frac{\Delta Z_{i,j}^{origin} - \Delta Z_{i,j}^{relaxed}}{\Delta Z_0}$ ,  $\Delta Z_{i,j}^{origin}$  is the distance between atoms  $i$  and  $j$  in unrelaxed slab,  $\Delta Z_{i,j}^{relaxed}$  is the distance between atoms  $i$  and  $j$  in relaxed slab,  $\Delta Z_0$  is the length of thickness of the surface slab.

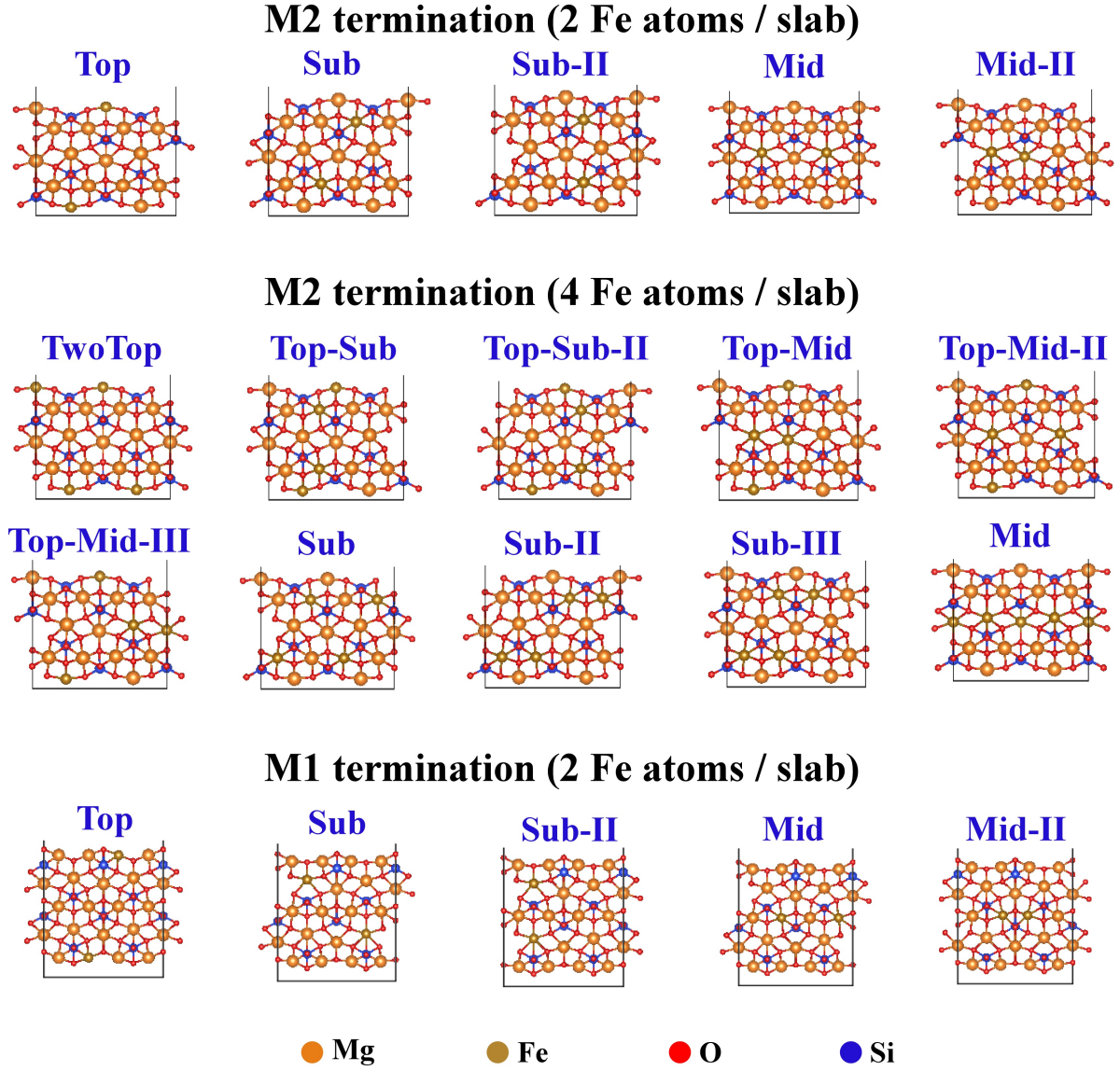


FIG. 5. Side Views of structures of the slabs with different Fe distribution and different terminations. M2 termination and M1 termination mean the slab have M2 or M1 site exposed on the surface respectively. The naming is based on the Fe atom location of the slab. Top means on the surface, Sub means under the surface, and Mid means inside the interior of the slab.

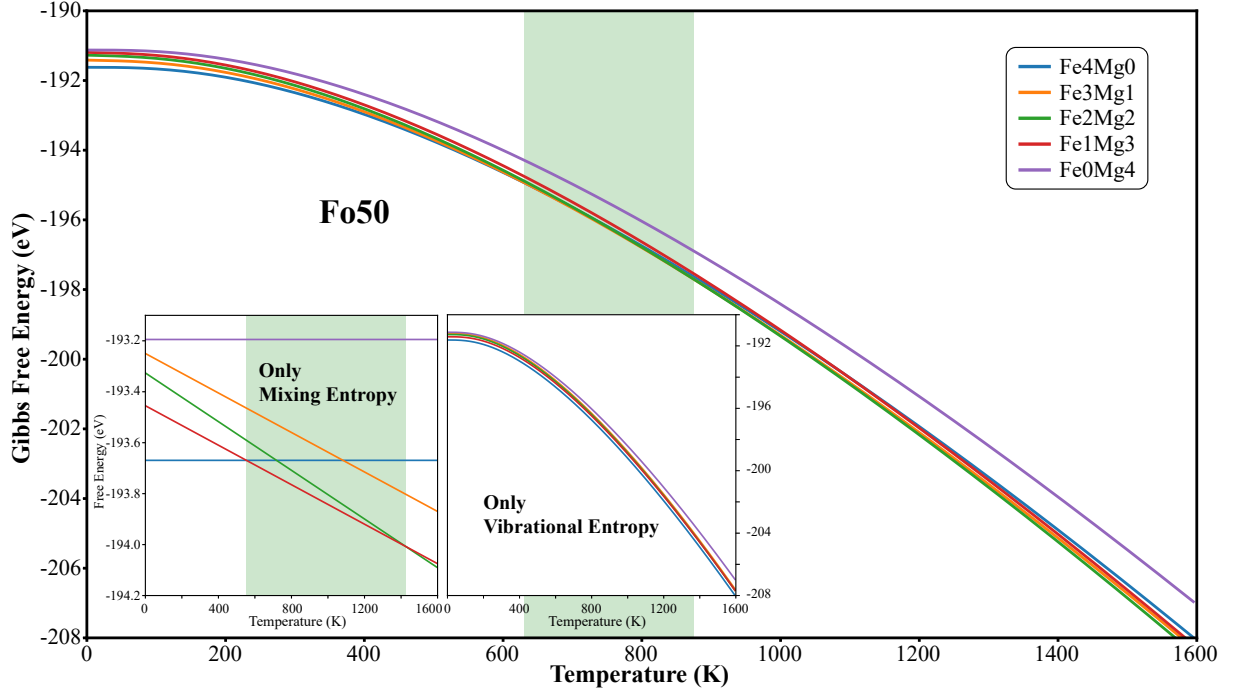


FIG. 6. Free energy comparison with different entropy contributions of Fo50. The shade span on the background is the energy crossover temperature range. Temperature below the crossover range the M1 ordered structure (Fe4Mg0) is the most stable, and above this range the fully mixed structure (Fe2Mg2) is most stable. Two Ordered structures have 0 mixing entropy contribution, so the energies are flat in the only mixing entropy graph. Only consider vibrational entropy the M1 ordered structure (Fe4Mg0) will always be the most stable structure.

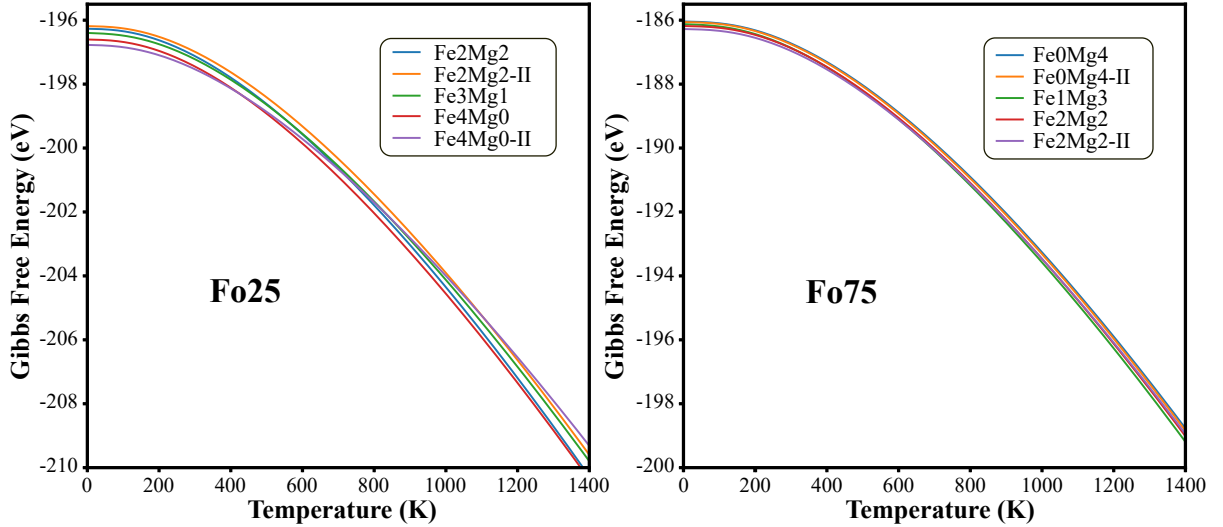


FIG. 7. Gibbs free energy comparisons of Fo25 and Fo75 structures. The crossover temperature changes with the composition variation, lower Fe content have lower crossover temperature and the structure which have the  $k_D = 1$  reaches the most stable above the crossover temperature.

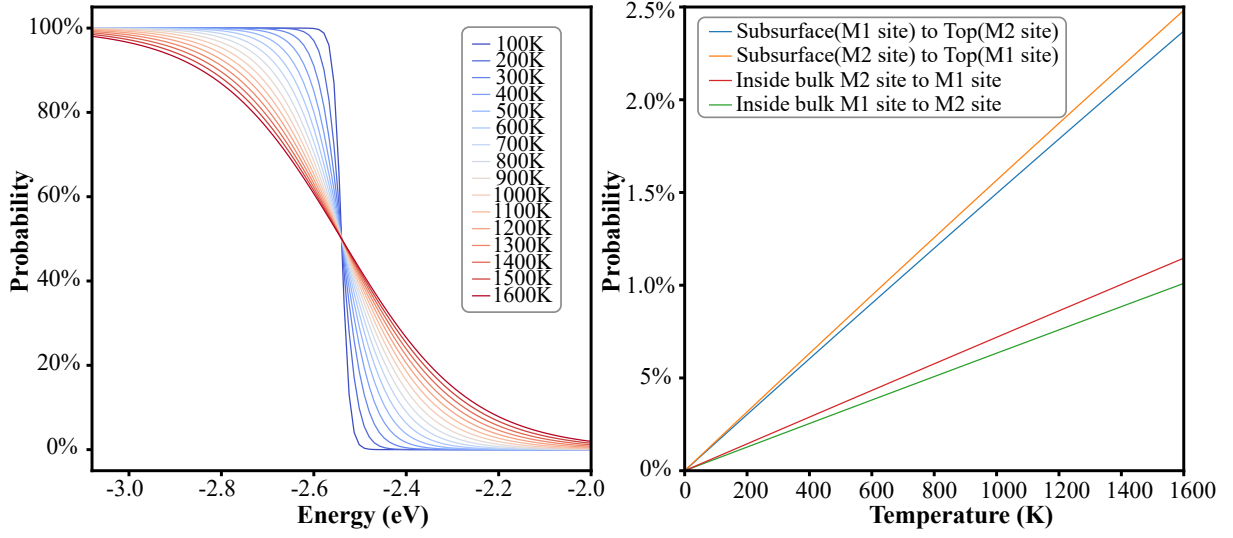


FIG. 8. Occupation probability estimation from a Fermi-Dirac distribution based on the energetics. We got the relative chemical potential of changing a Mg atom to a Fe atom from supercells results. From the estimation we can find the higher probability for Fe atoms moving from M2 site to M1 site in the bulk, and even higher probability if the Fe atoms are moving from the subsurface layer to the exposed metal site regardless of the type of the site. This would lead to a higher Fe concentration on the surface than in the bulk system after the diffusion of the Fe atoms.

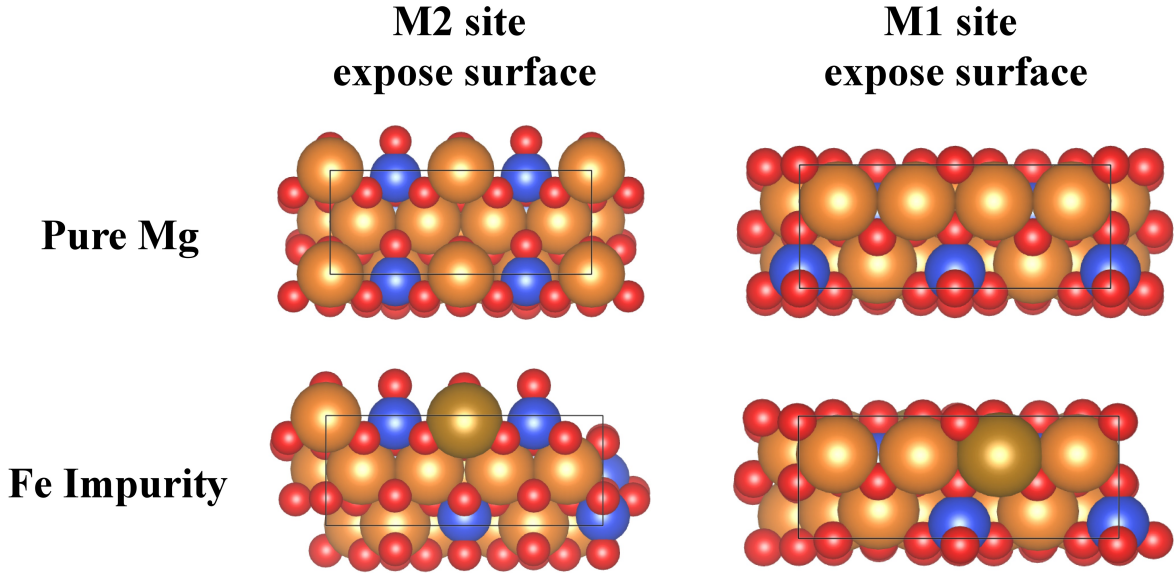


FIG. 9. Top view of possible slab structures with/without Fe atom.